CONF-970517--1
SAND--97-0309C SAN097-0309C

WET OXIDATION OF $AL_xGA_{1-x}AS$: ARSENIC BARRIERS ON THE ROAD TO MIS

Carol I.H. Ashby, John P. Sullivan, Paula P. Newcomer, Nancy A. Missert, Hong Q. Hou, B.E. Hammons, and Albert G. Baca
Sandia National Laboratories, Albuquerque, NM 87185-0603

ABSTRACT

Three characteristic regimes have been identified during the wet thermal oxidation of $Al_xGa_{1-x}As$ ($1 \geq x \geq 0.90$) on GaAs: 1) oxidation of Al and Ga in the $Al_xGa_{1-x}As$ alloy to form an amorphous oxide layer, 2) formation and elimination of elemental As (both crystalline and amorphous) and of amorphous As_2O_3, and 3) crystallization of the oxide film. Residual As can produce up to a 100-fold increase in leakage current and a 30% increase in the bulk dielectric constant. Very low As levels produce partial Fermi-level pinning at the oxidized $Al_xGa_{1-x}As$/GaAs interface. Local Schottky-barrier pinning of the Fermi-level at As precipitates at the oxide/GaAs interface may be the source of the apparent high interface state density. The presence of thermodynamically-favored interfacial As may impose a fundamental limitation on the application of AlGaAs wet oxidation for achieving MIS devices without post-oxidation processing to remove the residual As from the interface.

INTRODUCTION

There remains an unfulfilled need for an insulator with sufficiently low interface-state density to enable the GaAs-based equivalent of Si CMOS technology. The requisite low interface-state densities in the mid-10^{10} /cm^2-eV have not been obtained with dry thermal oxides and anodic oxides. Although very low interface-state densities have been obtained with MBE-grown Ga_2O_3 [1], a simpler and more cost-effective process is needed for large-scale device manufacturing. The possibility of forming readily manufacturable stable oxides suitable for metal-insulator-semiconductor (MIS) applications by oxidation of high-Al-content AlGaAs layers at elevated temperature during exposure to wet nitrogen [2] has been examined and preliminary efforts appeared promising [3]. With the goal of improving wet oxidation as a means of forming a good oxide, we have studied the temporal evolution of the composition and structure of oxidized AlGaAs films using Raman spectroscopy, x-ray diffraction, and electron microscopy. We have correlated these results with the electrical properties of the Al-oxide/GaAs materials system using DC transport and capacitance measurements. These studies have revealed a fundamental limitation on the application of AlGaAs wet oxidation for achieving MIS devices in the GaAs material system.

EXPERIMENT

Samples with the following structure were grown by MOCVD: 300 Å GaAs cap/ variable thickness $Al_xGa_{1-x}As$/1000 Å GaAs/GaAs substrate with x = 1.0, 0.98, and 0.90. Raman studies employed 0.25- and 2-μm $Al_xGa_{1-x}As$ layers, while diffraction (X-ray and electron) and bulk electrical measurements were performed on 0.25-μm $Al_xGa_{1-x}As$ samples. MIS capacitor samples for capacitance-voltage (C-V) measurements consisted of 300-500 Å of $Al_xGa_{1-x}As$ on 2-5x10^{16}/cm^3 n-GaAs and were grown by MOCVD or MBE.

Prior to wet oxidation, the GaAs cap was removed by a selective etch in a citric acid/peroxide mix [5:1 of (1g citric monohydrate/1g H_2O):30% H_2O_2] and the sample was loaded into the furnace under a dry nitrogen purge. The sample was then heated under flowing nitrogen.

DISCLAIMER

When the desired reaction temperature of 450 °C was reached, the nitrogen flow (typically 0.4 slm in a 2-in. diam. tube) was switched to bubble through water at a temperature of 80 ± 1 °C for a timed reaction. Dry nitrogen flow was restored at the completion of the reaction time and continued during sample removal from the furnace.

Raman spectra were measured using an excitation wavelength of 514.5 nm. The 500-mW probe beam was line focused to apply less than 85 W/cm^2 on the sample. Scattering was measured in the $x(y',y'+z')\bar{x}$ backscattering configuration with y' and z' parallel to (110) planes. A triple monochromator with an internal depolarizer and a CCD array detector were employed. Reference Raman spectra were obtained for α-Al_2O_3 (99.997%, 110 μm crystalline, 9 m^2/g surface area) and γ-Al_2O_3 (99.999%, 110 μm powder, 55 m^2/g surface area). Peak positions in cm^{-1} and relative intensities for α-Al_2O_3 were as follows: 379 (0.34), 417(1), 428(0.28), 458(0.06), 576(0.11), 644(0.24), 750(0.23). Weak Raman peaks from γ-Al_2O_3 were observed at 385, 468, 624, 644, 750 cm^{-1}. This small crystallite size might cause red-shifting and asymmetric broadening of the peaks [4]; low signal intensity prevented evaluation of this possible effect.

X-ray diffraction measurements were performed on the films using Cu K-alpha radiation from a fixed anode source and a curved graphite crystal detector. Conventional Θ-2Θ scans were taken between 10° and 70°, corresponding to lattice spacings of 8.8 Å-1.34 Å. X-ray measurements on γ-Al_2O_3 showed a broad amorphous background with broad peaks; using the Scherrer formula gives a crystallite size of 70 Å.Cross-section samples for high resolution transmission electron microscopy (TEM) were prepared by mechanical thinning and ion milling with 5 kV Ar^+ and examined at 200 keV using a JEOL 2010 at the University of New Mexico.

Samples for electrical characterization were prepared by shadow mask deposition of Ti/Au circular contacts (200-1000 μm) on the oxide surface followed by deposition of a non-alloyed ohmic backside contact. For bulk dielectric measurements, 0.25 μm thick oxidized $Al_xGa_{1-x}As$ layers on top of near-degenerately n-doped GaAs were used in order to minimize the interfacial depletion layer capacitance. For interface electrical characterization, thinner $Al_xGa_{1-x}As$ layers were measured on 2-5x10^{16} cm^{-3} n-doped GaAs buffer layers. C-V measurements were performed over the frequency range 100 kHz to 1 MHz, typically 1 MHz, at a sweep rate of 150 mV/min. DC transport measurements were performed over the range -5 V to 5 V under dark conditions.

RESULTS AND DISCUSSION

As the oxidation front moves deeper into the original AlGaAs layer, the AlAs-like phonon peak intensity at 400 cm^{-1} is reduced, as shown in Fig. 1 for a 2-μm $Al_{0.98}Ga_{0.02}As$ layer. Substrate GaAs is observed at 292 cm^{-1} due to the low absorption coefficient of indirect-gap $Al_{0.98}Ga_{0.02}As$ at 514.5 nm. The Raman spectrum of a partially oxidized film is dominated by crystalline As peaks at 198 and 257 cm^{-1} and by a broad feature between 200 and 250 cm^{-1} peaking near 227 cm^{-1} ascribed to amorphous As [5]. The As peaks are very strong due to resonant enhancement of the Raman scattering at this excitation energy; the detection limit is on the order of 10- to 20-Å layers [6]. The broad feature centered at 475 cm^{-1} is due to amorphous As_2O_3 [6]. Specific peaks associated with amorphous Al-oxides are neither expected nor observed in these thin films. Gallium oxide films of 8000-Å thickness are not detectable by Raman because of low cross section [6], and the less polarizable Al-oxide films should be even weaker scatterers.

A relatively constant Raman signal from As and a-As_2O_3 is obtained during most of the oxidation while the intensity of the AlAs-like phonon decreases (Fig 1a-c.) as the oxidation front advances into films of either AlAs or high-Al-fraction AlGaAs. Oxidation of Al(Ga)As to an amorphous Al(Ga)-oxide film is manifested by the gradually rising baseline. As the oxidation front approaches the GaAs interface, the AlAs-like phonon peak intensity falls below our detection limit. The a-As_2O_3 peak intensity also falls below the detection limit. Barely detectable scattering from As and a steeply rising baseline remain (Fig. 1d). Continued exposure to the oxidizing atmosphere or annealing in vacuum or dry nitrogen leads to crystallization of the film (Fig. 1e); most of the strong peaks in Fig. 1e are from Rayleigh scattering of laser-plasma light or from GaAs-associated features observed on rough GaAs, where polarization selection rules that are operative with specular surfaces break down. Weak peaks at 750 and 644 cm^{-1} ascribed to γ-Al_2O_3 are observed in 2.0-μm crystallized films. Delamination of the 2.0-μm films routinely occurs upon crystallization, suggesting relatively weak adhesion between the oxide and semiconductor. This is consistent with the relative fragility of laterally oxidized optoelectronic structures when subjected to cleaving operations.

We propose the following reaction scenario for Al(Ga)As films undergoing wet oxidation. Al(Ga)As undergoes reaction with water, hydroxyl, or other oxygen-containing species derived from water to form a mixture of aluminum(gallium) oxides and/or hydroxides and amorphous As_2O_3, which forms a glassy matrix and prevents wide-scale crystallization. Elemental As is present at a relatively constant amount throughout most of the oxidation. This amount is determined by the kinetic balance between its formation and subsequent loss through further oxidation or volatilization and escape through the permeable oxide film; this balance will vary with specific reaction conditions such as temperature and gas flow rates. TEM studies of laterally wet-oxidized AlGaAs layers have shown the oxide layer to be far from fully dense; it should have adequate permeability for ready escape of volatile reaction products [7]. Both As [P(vap) = 760 Torr at 407 °C] and a-As_2O_3 [P(vap) = 760 Torr at 320 °C] could be the vehicle for removal of As from the growing oxide film. Arsine has been postulated as the major product of AlGaAs wet oxidation. We cannot rigorously exclude a role for arsine as a product, since our furnace was not equipped for collection and identification of volatile products. However, our observation of two volatile As-species in more highly oxidized states than the original AlGaAs suggests that formation of major quantities of the lower oxidation state arsine as the volatile reaction product is unnecessary for As removal from the oxidized film.

Figure 2 shows high-resolution TEMs of the interfacial region between $Al_{0.90}Ga_{0.10}As$ and GaAs as the oxidation front approaches the interface. Moiré fringes due to a 2-4 nm crystallite at the interface and lattice fringes associated with unreacted $Al_{0.90}Ga_{0.10}As$ are observed near the oxide/GaAs interface. Selected area diffraction taken within the oxidized $Al_{0.90}Ga_{0.10}As$ layer show diffuse polycrystalline rings with d-spacings corresponding to the prominent reflections of γ-Al_2O_3. X-ray diffraction measurements on similar films reveal only a diffuse background with no apparent crystalline Al_2O_3 phases, thus putting an upper limit on crystallite size of ~ 10 nm. Crystallite sizes ranging from 1 to 13 nm were seen in the laterally oxidized TEM study, with most grains being approximately 4 nm in diameter [7]. The lower magnification image of Fig. 3 reveals that the interfaces are not abrupt, but exhibit interfacial roughness on the order of 2-4 nm.

The evolution of the structure of these surface-oxidized films correlates with that observed along the length of a laterally-oxidized buried layer [7]. At the oxide/semiconductor interface of a laterally oxidized layer, an amorphous region is observed. Farther back from the oxidation front, the oxidized layer becomes increasingly crystalline (γ-Al_2O_3). Since increasing distance from the

oxidation front in a laterally oxidized sample correlates with increasing oxidation time, the evolution from amorphous to crystalline structures in both laterally and surface-oxidized samples is probably due to progressive loss of the stabilizing glassy matrix provided by a-As_2O_3 or to conversion of amorphous Al_2O_3 to crystalline γ-Al_2O_3.

Table 1 summarizes the results of capacitance and DC transport measurements on 0.25-μm wet-oxidized films as a function of residual As and Ga content. "High" arsenic samples exhibit As Raman signals on the order of those shown in Fig. 1a-c while "low" arsenic samples exhibit As signals below the Raman detection limit. Residual As can produce nearly a 100-fold increase in leakage current and up to a 30% increase in the dielectric constant. The increase in dielectric constant with increasing As concentration may be partly due to dielectric heterogeneity associated with metallic As precipitates in the insulating aluminum oxide matrix. Assuming that As precipitates produce the entire increase and adopting a Maxwell-Wagner form for the effective dielectric constant [8], the required volume fraction of elemental As would be approx. 6% for the high As content oxidized AlAs layer. The increase in bulk dielectric constant with increasing Ga content is probably due to the greater polarizability of Ga-O versus Al-O bonds. The dielectric constant of deposited Ga_2O_3 films has been reported to be up to 14.2 [1].

C-V measurements on thin oxidized $Al_xGa_{1-x}As$ layers (Fig.3) with residual As at levels below the Raman detection limit (≈ 10- to 20-Å layers) [6] reveal partial Fermi-level pinning with weak C-V modulation while measurements on layers with higher As content exhibit strong Fermi-level pinning and no modulation. The failure to reach full-accumulation capacitance in the low-As samples would be consistent with the existence of an interface-state band located approximately 0.3 to 0.6 eV below the GaAs conduction band (CB) with a state density exceeding 10^{12} cm^{-2}. It is possible that local pinning of the Fermi-level at As precipitates near the oxide/GaAs interface may be the source of the apparent high interface state density. The Schottky barrier height observed for an As/n-GaAs interface is 0.67 - 0.72 eV [9], which would appear as an apparent interface-state band below the level found here. However, if the As precipitates do not fully cover the oxide/GaAs interface, a situation may arise in which the Fermi-level at the interface may only be pinned in close proximity to As precipitates and may be unpinned in intervening regions free of As. The observed pinning positions of 0.3 to 0.6 eV below the GaAs CB may, therefore, be explained alternatively by non-uniform Fermi-level pinning at As crystallites at the interface (e.g., the formation of local barriers) with an areal coverage of As at the interface between 83 and 98%. This non-uniform pinning of the Fermi-level at the oxide/GaAs interface would prevent the formation of a spatially uniform accumulation layer near the oxide interface and could explain the low transconductance observed in field effect transistor (FET) devices employing oxidized $Al_xGa_{1-x}As$ gates.[3].

One should expect to find some residual As at the oxide/GaAs interface even after lengthy oxidation based on thermodynamic considerations [10] when As_2O_3 is an oxidation product, as we observe. Even if the As formed from Al(Ga)As oxidation were totally removed, further generation of interfacial As from oxidation of GaAs could proceed from the reaction

$$2\ GaAs + As_2O_3 = 4\ As + \beta\text{-}Ga_2O_3 \qquad \Delta G^0_f = -64\ kcal/mole \quad (1).$$

Since interfacial As even at the 10^{-4} monolayer level will degrade MIS performance, this poses a serious problem for achieving a viable GaAs MIS technology based on wet oxidation alone.

SUMMARY

Both elemental As and amorphous As_2O_3 form during AlGaAs wet oxidation. Their high vapor pressure at normal oxidation temperatures is sufficient for them to be the primary species that transport arsenic out of the relatively porous oxidized film. Elemental As is present in both crystalline and amorphous forms, with crystalline As requiring a longer reaction time for removal than amorphous As after the oxidation front reaches the substrate GaAs. Thick (2-μm) Al-oxide films crystallize and delaminate after As and a-As_2O_3 are removed by continued oxidation and/or heating. The relatively weak adhesion between the oxide and the underlying GaAs following surface oxidation may be responsible for the fragility of some laterally oxidized optoelectronic structures. Both capacitance-voltage and DC transport behavior are degraded by the interfacial As. Non-uniform pinning of the Fermi-level at the oxide/GaAs interface by As precipitates may explain the partial Fermi-level pinning and low transconductance of FET devices. Good MIS devices will require As removal without film crystallization. However, the fundamental limit imposed by the thermodynamically favored formation of elemental As at the oxide/GaAs interface makes this a formidable challenge.

This work was performed at Sandia National Laboratories and supported by the U.S. Department of Energy under Contract No. DE-AC04-94AL85000. Sandia is a multiprogram laboratory operated by Sandia Corporation , a Lockheed Martin Company, for the United States Department of Energy.

REFERENCES

[1] M. Passlack, M. Hong, J. P. Mannaerts, Appl. Phys. Lett. 68, 1099 (1996).
[2] J.M. Dallesasse, N. Holonyak, Jr., A.R. Sugg, T.A. Richard, and N. El-Zein, Appl. Phys. Lett. 57, 22844 (1990).
[3] E.I.Chen, N.Holonyak, Jr., and S.A Maranowski, Appl. Phys. Lett. 66, 2688, (1995).
[4] H. Richter, Z.P. Wang, L. Ley, Solid State Comm. 39, 625 (1981).
[5] G.P. Schwartz, B. Eschwartz, D. DiStefano, G.J. Gualtieri, and J.E. Griffiths, Appl. Phys. Lett. 34, 205 (1979).
[6] G.P. Schwartz, G.J. Gualtieri, J.E. Griffiths, C.D. Thurmond, B. Schwartz, J. Electrochem. Soc. 127, 2488 (1980).
[7] R.D. Twesten D.M. Follstaedt, K.D. Choquette, and R.P. Schneider, Jr. Appl. Phys. Lett. 69, 19 (1996).
[8] B. K. P. Scaife, Principles of Dielectrics (Clarendon Press, Oxford, 1989.)
[9] J.M. Woodall, P.D. Kirchner, J.F. Freeouf, D.T. McInturff, M.R. Melloch, F.H. Pollak, Phil. Trans. Roy. Soc. Lond. A 344, 521 (1993).
[10] C.D. Thurmond, G.P. Schwartz, G.W. Kammlott, and B. Schwartz, J. Electrochem. Soc. 127, 1366 (1980).

Table 1: Bulk Electrical Properties of Wet-Oxidized AlGaAs Films

Starting Composition	Arsenic	Leakage (A/cm^2 @ 5V)	Bulk Resistivity (Ohm-cm)	Bulk Dielectric Constant (1MHz)
AlAs	Low	$7.5x10^{-8}$	$2.7x10^{12}$	5.8
	High	$7.5x10^{-7}$	$2.7x10^{11}$	7.0
$Al_{0.98}Ga_{0.02}As$	Low	$2.9x10^{-9}$	$6.9x10^{13}$	6.2
	High	$2.5x10^{-7}$	$8.0x10^{11}$	8.3
$Al_{0.90}Ga_{0.10}As$	Low	$3.7x10^{-9}$	$5.4x10^{13}$	8.6
	High	$1.0x10^{-7}$	$1.2x10^{11}$	8.2

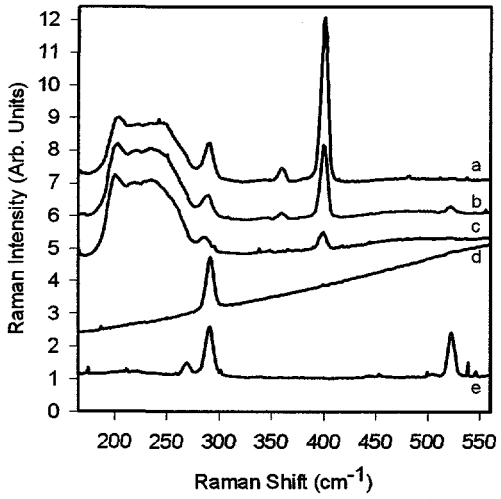

Fig. 1: Raman spectra of progressively oxidized 2.0-μm layer of $Al_{0.98}Ga_{0.02}As$ on GaAs: a-c) partially oxidized; d) oxidized "to completion"; e) layer crystallized and delaminating.

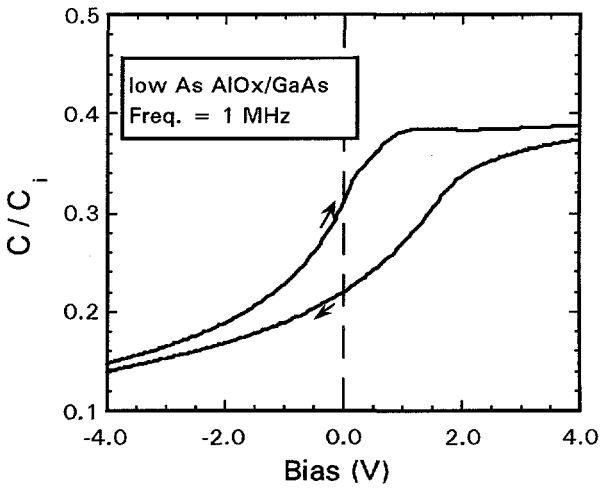

Fig. 3: Capacitance-voltage (C-V) curve for a low-As MIS capacitor with 300-Å of oxidized AlAs on 2 x 10^{16} cm^{-3} n-GaAs showing weak C-V modulation (deep depletion seen at large inversion bias).

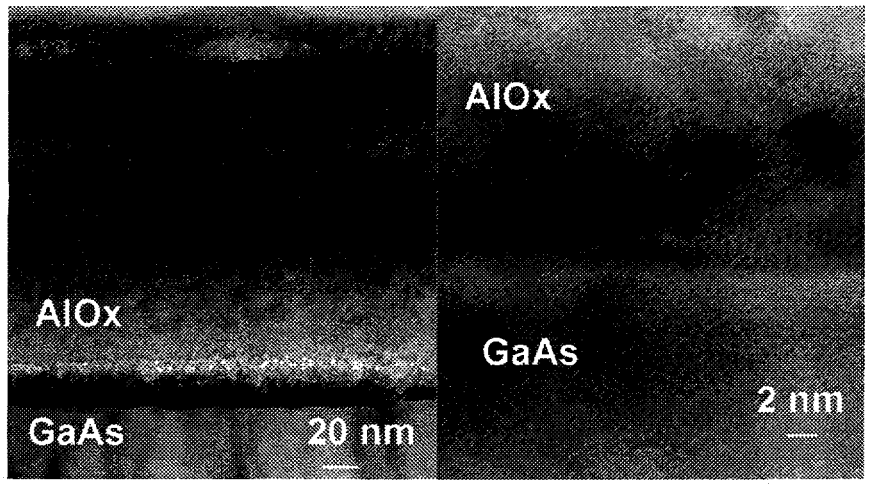

Fig. 2: High-resolution transmission electron micrograph of interfacial region of oxidized $Al_{0.90}Ga_{0.10}As$ as oxidation front approaches GaAs. Arsenic precipitates (2-4 nm) present at interface.